APL Materials

Strategies to improve the photoelectrochemical performance of hematite nanorod-based photoanodes

Cite as: APL Mater. **8**, 040905 (2020); https://doi.org/10.1063/5.0003146
Submitted: 01 February 2020 . Accepted: 24 March 2020 . Published Online: 07 April 2020

Aryane Tofanello, Shaohua Shen, Flavio Leandro de Souza, and Lionel Vayssieres

Strategies to improve the photoelectrochemical performance of hematite nanorod-based photoanodes

Cite as: APL Mater. 8, 040905 (2020); doi: 10.1063/5.0003146
Submitted: 1 February 2020 • Accepted: 24 March 2020 •
Published Online: 7 April 2020

Aryane Tofanello,[1,2,a)] Shaohua Shen,[1] Flavio Leandro de Souza,[2,3,a)] and Lionel Vayssieres[1,a)]

AFFILIATIONS

[1]State Key Laboratory of Multiphase Flow in Power Engineering, School of Energy & Power Engineering, International Research Center for Renewable Energy (IRCRE), Xi'an Jiaotong University, Xi'an 710049, China
[2]Centro de Ciências Naturais e Humanas (CCNH), Federal University of ABC (UFABC), Santo André 09210580, Brazil
[3]Brazilian Nanotechnology National Laboratory (LNNANO), Brazilian Center for Research in Energy and Materials (CNPEM), Campinas 13083-970, Brazil

[a)]**Authors to whom correspondence should be addressed:** aryane.tofanello@ufabc.edu.br; flavio.souza@ufabc.edu.br; and lionelv@xjtu.edu.cn

ABSTRACT

An overview on the recent progress in experimental strategies used to improve the photoelectrochemical response of hematite nanorod-based photoanodes for solar water splitting is provided. Emerging areas are identified that will require attention as the search continues for stable and efficient visible-light driven water oxidation systems that exploit the rational construction of different interface junctions. Increasing efforts have been focused on enhancing the performance of hematite-based photoanodes via morphology control, element doping, co-catalysts, surface modification, heterojunction construction, and via a combination between them. Particular attention has been given to heterojunctions, as these structures are more likely to utilize the benefits provided by combining elements with distinct properties, exhibiting functional behavior at the interfacial region, and increasing solar energy conversion by synergistic effects.

I. INTRODUCTION

Rapid economic and demographic growth has driven the rise in world consumption of clean energy in an attempt to curb the disastrous effects of pollution for our health and environment. Among the options, solar energy has become a great alternative, although its large-scale applicability is still limited. In the pursuit of the most applicable photoanode for photoelectrochemical (PEC) water splitting, hematite (α–Fe_2O_3) has attracted interest for a few decades.[1–4] This can be explained in part because hematite can theoretically collect up to 40% of the solar spectrum [exceeding the minimum solar-to-hydrogen (STH) efficiency for practical applications], and it shows excellent photoelectrochemical stability over a wide pH range, including its practical use in seawater, suitable energy band gap (1.9–2.2 eV) for light harvesting; in addition, its main constituent, iron, is the fourth most abundant element in the Earth. However, several intrinsic factors limited the hematite water oxidation activity, including poor electrical conductivity, high charge recombination rates, slow charge transfer kinetics at the electrode/electrolyte interface, low reaction kinetic oxygen evolution, and short hole diffusion length, among others.[5–7] These limitations, which may occur in the bulk and at the surface, lead to multiple electron–hole recombination pathways that significantly decrease the PEC performance of hematite photoanodes, and reported efficiencies in practical applications and devices are noticeably lower than the predicted theoretical value.[5–7] The photocurrent density (J_{PEC}), which can be described by Eq. (1), is commonly known as the absorbed photocurrent density (J_{abs}) and the global photocurrent conversion efficiency, which is the product of the charge carrier separation efficiency (η_{sep}), representing the fraction of holes reaching the semiconductor/electrolyte

interface without recombining with electrons in the bulk, and the injection efficiency (η_{inj}) for water oxidation, representing the fraction of holes for a desired oxidation reaction without recombining with electrons at the surface. Thus, in a simplified way, parameters may change depending on the type of hematite engineering in an attempt to have a positive balance when they act together,[8,9]

$$J_{PEC} = J_{abs} \, X \, \eta_{sep} \, X \, \eta_{inj}. \quad (1)$$

It is interesting to note that the parameters involved in the overall photoelectrochemical response are actually coupled with each other. For instance, increasing J_{ABS} achieved by morphological changes can often result in an increase in surface states promoting charge recombination at the interfaces. Thus, it is mandatory to emphasize that the nanoscale morphological design of hematite photoelectrodes has become one of the most important parameters to be first controlled in order to boost the electronic properties and facilitate the water oxidation reaction kinetics, reducing the electron–hole recombination rate. For many years, the anisotropic (i.e., columnar) structure (so-called hematite nanorods) has been established as the most appropriate, as a consequence of nanometric dimensions coupled with the shortened hole diffusion length, higher surface area as well as an increased tunability of electronic states (changing the dynamics of photogenerated carriers) due to quantum confinement. When the nanorods have their dimensions comparable to carrier diffusion lengths, the holes are able to easily access the surface, facilitating their extraction at the interfaces, as seen in the schematic comparison of the diffusion patterns of charge carriers between a hematite nanorod array and a spherical hematite array [Fig. 1(c)]. Figures 1(a)–1(c) show a simplified representation of changes in electronic states, electron mobility, and charge transfer path in a 1D hematite (nanorods) array, respectively.[10,11]

It is known that electrical conduction in crystalline lattices is guided by two main mechanisms: a band or tunneling process, which occurs at low temperature and an activated hopping process, which dominates at high temperature.[12] Given that charge conduction takes place via hopping mechanism in hematite nanostructures and the annealing temperature is closely related to its crystallinity, the adjustment of the crystallinity can lead to a reduction in the structural defects, which are identified as the main causes of recombination in hematite photoanodes. Thus, because it is usual to anneal hematite for PEC applications at high temperatures, it is frequent to increase its photoactivity due to the improvement of the crystalline structure (with minimal charge trapping defects) and reduction of defects in the solid/solid interface, as well as in the bulk and surface of hematite.[13–16] When considering a structure of hematite nanorods thermally treated at high temperatures in short times, its distortion and coalescence is avoided, the effective surface area is increased and the crystallinity is improved by decreasing bulk defects, making the charge separation effective as well as charge transfer at the electrode/electrolyte interface.[17] Thus, arrays of hematite nanorods oriented vertically to the conductive substrate are significant to facilitate the collection of photogenerated electrons and to further boost

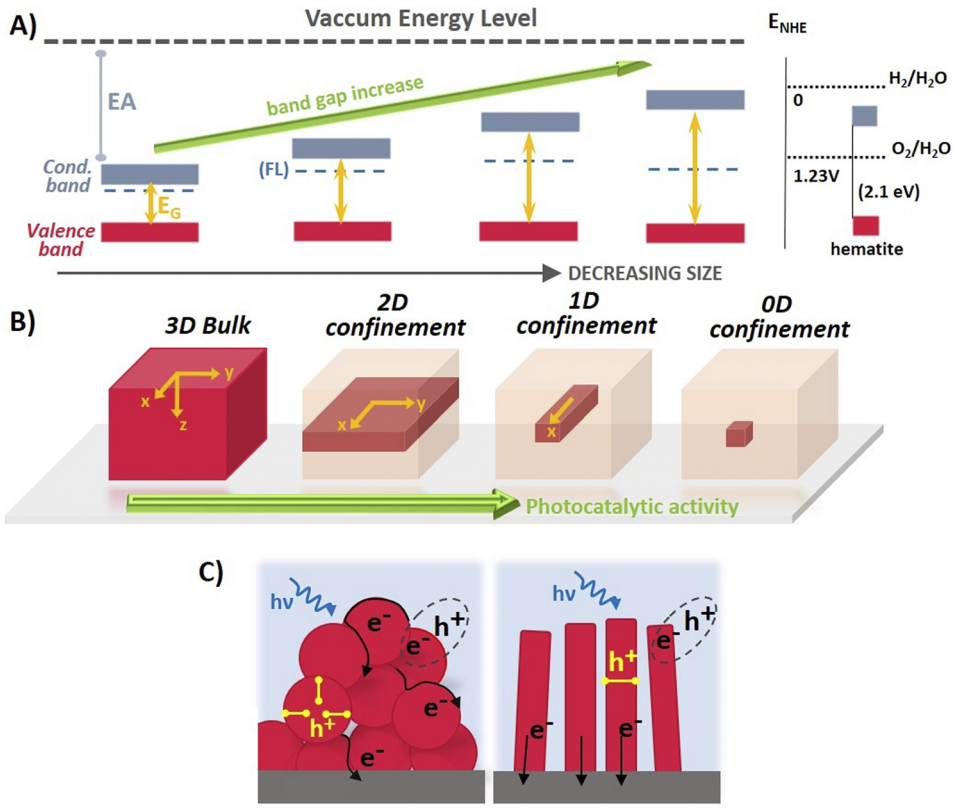

FIG. 1. Schematic diagram showing the effect of quantum confinement (a) on a hematite electronic structure (EA = electron affinity, FL = Fermi level, and E_G = band gap): conduction band expansion to achieve redox energy of the H^+/H^{2+} level, (b) electron mobility in different dimensions (x, y, and z) on 0D, 1D, 2D, and 3D structures, and (c) comparative behavior of charge carrier transport in a spherical hematite nanoparticle array (left) and in a hematite nanorod array (right). The charge diffusion patterns are highlighted in yellow for holes and black for electrons.

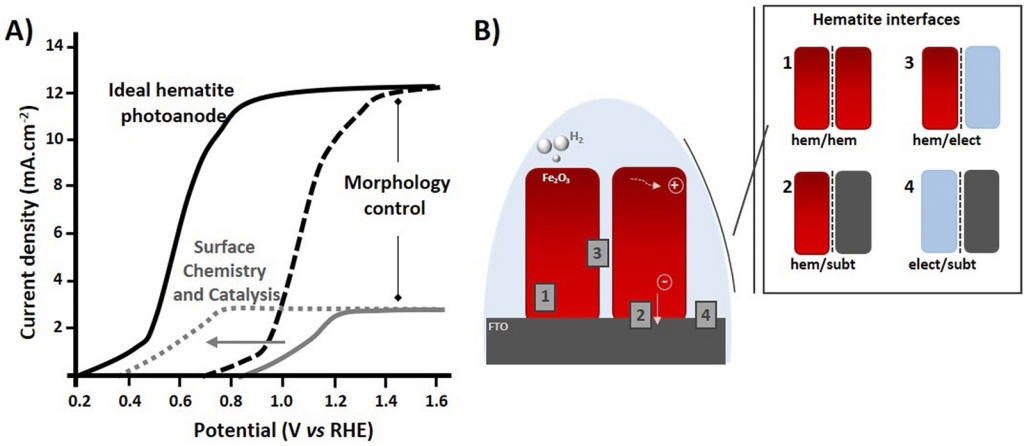

FIG. 2. (a) Hypothetical profile of PEC response for an ideal hematite photoanode (solid black line) compared to a typical photoanode (solid gray line) with the expected effects after rational arrangement of interfaces. (b) Schematic illustration of main charge recombination interfaces in hematite-based photoanodes: (1) hematite/hematite, (2) hematite/substrate, (3) hematite/electrolyte, and (4) electrolyte/substrate.[33,34] (a) Adapted with permission from Sivula *et al.*, ChemSusChem **4**, 432–449 (2011). Copyright 2011 WILEY-VCH Verlag GmbH & Co. and (b) Adapted with permission from Soares *et al.*, Phys. Chem. Chem. Phys. **18**, 21780–21788 (2016). Copyright 2016 Royal Society of Chemistry.

the PEC efficiency, as previously discussed. Combined with the crystallinity achieved by annealing, this system provides a strategy that facilitates the charge migration and allows the photogenerated holes to reach the electrolyte interface efficiently, facilitating the water oxidation.

Figure 2 illustrates the main observed recombination paths from 1 to 4, as highlighted in the inset, associated with bulk losses (number 1), in the in solid–solid interface (number 2), and in the solid–liquid interface (numbers 3 and 4). Improving bulk losses (number 1) by adjusting the morphology, it is still possible to identify from Fig. 2(b) the main electron–hole recombination pathways that can occur in the solid–solid (number 2) and solid–liquid (numbers 3 and 4) interfaces. Still according to Eq. (1), modifications must be designed to have a balance that optimizes η_{sep}, η_{inj}, and J_{abs} and to minimize the deleterious effects presented by each interface, seeking the rational arrangement of interfaces to achieve the ideal J_{PEC} curve.[18–20] In general, rational strategies proposed to overcome the hematite limitation toward efficient solar water splitting are based on the development of new nanostructured interface architectures to reduce charge recombination, ion doping in crystalline structures to increase conductivity, surface passivation to avoid recombination and promote better charge transfer, and use of co-catalysts or surface modification with a secondary semiconductor to improve water oxidation kinetics.[1,21–25] Providing a very promising way to optimize solar-to-hydrogen (STH) efficiency, many research groups worldwide are already using heterojunction engineering (using co-catalysts, innovative hierarchies, plasmonic structures, dopants, etc.) to develop more efficient photoelectrodes.[26–31] Although Jeon *et al.* achieved the highest PEC efficiency using elaborately designed hematite arrays, with a current density of 6 mA cm^{-2} at 1.23 V vs reversible hydrogen electrode (RHE), this value is still far from the theoretical limit for hematite.[32] Having defined the main concepts and limiting parameters of PEC water splitting, in this perspective, we will highlight the current progress over the years in the improving photocurrent in relation to rationalization of hierarchical interface engineering. Some more current strategies, such as heterojunctions, will be discussed more extensively due to their benefits. Finally, after presenting a wide range of technologies applicable to hematite nanorod-based photoanodes, some future technology directions for hematite-based photoanodes will be discussed.

II. RECENT STRATEGIES TO OVERCOME THE SURFACE LIMITATIONS OF HEMATITE NANOROD-BASED PHOTOANODES AND IMPROVE THEIR PEC PERFORMANCE

Before discussing the effectiveness of any strategy proposed to overcome the hematite limitation, it is worth noting that their response is not completely independent. This means that there are certainly some strategies that change more than one efficiency parameter concomitantly. However, this work focuses on the performance metric that is most affected in the system by each strategy with respect to the theoretical perspective. It is also important to point out that the effects of intrinsic modification engineering (annealing temperature, atmosphere, and acid/base treatments on surface-charge properties) will not be addressed in this perspective, but can be better understood in some excellent literature reports on PEC water splitting.[33–38]

A. Elemental doping

Among the various strategies applied to improve the overall efficiency of a hematite-based photoelectrode, the insertion of a doping element is the one that has been the most explored. Heteroatoms with diverse atomic radii and valence electrons, when incorporated into a semiconductor lattice, have been considered as an effective method for mainly regulating the electrical conductivity through

the decrease in the minority carrier concentration with a beneficial effect on V_{onset}, among other contributions.[39–48] Among the most commonly used elements for doping hematite photoelectrodes to improve the conductivity and carrier mobility are the tetravalent Sn, Ti, and Si.[49–51] A published work showed that Sn^{4+} doping in hematite photoanodes increased the photocatalytic response because the tin induced a superficial donor level below the hematite conduction band.[47] The Sn^{4+} ion generated a local microstrain in the lattice, decreasing the Fe–O bond ordering, introducing electrons to Fe^{3+} sites (which are reduced to Fe^{2+}), and, consequently, improving the electrical conductivity. Interestingly, recent work by Hufnagel *et al.* systematically evaluated the advantages and limitations of controlled Sn doping at the surface, in the subsurface volume, and in the bulk of hematite photoanodes.[48] In summary, Sn doping facilitated the separation of photogenerated electron–hole pairs, increasing the efficiency of charge separation, while surface ions played a dual role in eliminating surface states, preventing hole trapping and decreasing the overpotential. More recently, fundamental investigations reported by several research groups have provided a novel perspective and somehow a deeper understanding of the role of Sn^{4+} incorporation in hematite-based material. By performing electrical and thermomechanical measurements in undoped and Sn-doped hematite nanoscale powders annealed at different temperatures and controlled oxygen partial pressure atmosphere, Wang *et al.* could derive the impact of the defect chemistry in such systems.[52] In fact, using the equilibrium defect models and monitoring several parameters during the *in situ* electrical measurement, the authors interestingly found a weak or negligible impact of Sn-addition on the donor density number and overall electrical conductivity. In a similar context, Soares *et al.* investigated undoped and Sn-doped hematite annealed at fixed temperature and designed on purpose with controlled number of interfaces, showing that the presence of Sn led to the decrease in the grain boundary resistance favoring the electron transport through the doped interfaces.[53] In another report, the authors doped hematite photoanodes with Sn *ex situ* through atomic layer deposition (ALD).[51] The SnO_x ALD still occurred in the form of FeOOH nanorods to facilitate the dopant diffusion into the semiconductor lattice. Thus, after annealing treatment, it was observed that the SnO_x layer reduced surface defects, improved carrier conductivity, and provided protection, and the system exhibited an exceptional performance of 3.12 mA cm^{-2} at 1.23 V vs RHE. After identifying that different hematite doping routes had already been investigated under different conditions, Guo's group reported the effect of seven dopants on the structural, electrical, and photoelectrochemical properties of the hematite film under the same experimental conditions.[54] In summary, from the results of the Mott–Schottky and electrochemical impedance spectroscopy (EIS), they showed that the improvement of PEC performance of doped hematite is mainly due to the positively shifted flat band potential, which changes the surface states and interface charge transport property. Unlike other previous findings, they reported that doping had a slight influence on the charge carrier densities.[55] Since building heterojunctions or inserting co-catalysts or other nanostructures on hematite photoanodes may introduce some new interfaces with carrier traps and recombination centers, emerging strategies have been proposed to accelerate charge separation involving sequential dopant incorporation, whether metallic or non-metallic ions, or bimetallic doping.[56,57] In this study, it was possible to modulate the low carrier density and high charge recombination of hematite photoanodes by co-modification, adjusting the annealing temperature and the ion incorporation into the hematite lattice.[58] A substantially superior photocurrent of 2.56 mA cm^{-2} and a cathodic shift of V_{onset} (~90 mV), which can be observed in Fig. 3(a) by the co-doped P–Ti–Fe_2O_3 photoelectrode, were achieved after initial Ti-modification (calcination at 800 °C) followed by P-additional modification (calcination at 350 °C) due to decreased surface trap states, which improved the charge carrier density. It was reported that the annealing temperature and doping mechanisms, in an optimized and synergistic mechanism, influenced the hematite PEC performance, increasing the carrier density, as manifested by the Mott–Schottky plot in Fig. 3(b), improving the electrical conductivity and facilitating the charge carriers transfer. The charge separation efficiency (η_{sep}) and charge injection efficiency (η_{inj}) are shown in Figs. 3(c) and 3(d), in which the separation efficiency is still a limiting factor in the PEC performance, with its best value obtained by the P–Ti–Fe_2O_3 photoelectrode (approximately 20%). However, the same system had the hole injection efficiency of almost 100% at 1.23 V vs RHE, outperforming the other systems analyzed which explained its considerable photocurrent enhancement. This study reinforces the need to combine different elements and conditions of synthesis and annealed treatment to achieve an improved overall efficiency in hematite-based photoelectrodes.

Most recently, Zhu *et al.* reported a beneficial effect for the Ti and Zn dual-doping case, in which titanium ions were introduced into the hematite still in the hydrothermal process, while zinc was incorporated by dipping–sintering treatment, forming the Ti and Zn co-doped hematite.[46] Their EIS data and density functional theory (DFT) calculations showed that while the enhancement aroused by Ti doping was attributed to increased carrier density and higher charge separation efficiency, the Zn dopant reduced the electron–hole recombination in the bulk and at the surface of the photoelectrode. With a simple electrochemical activation treatment (repeated reduction and oxidation processes), which modified both the surface and bulk properties, Zhang *et al.* proved that co-doped hematite Nb,Sn:Fe_2O_3 applied to this surface and bulk activation condition showed an effective improvement in PEC performance.[59] The modifications ensured fewer defects and richer Nb–O and Sn–O bonds to hematite, passivating surface trap states and improving its PEC stability. Adopting a hybrid microwave annealing (HMA) treatment to incorporate Nb and Sn atoms into the hematite lattice, Figs. 4(a)–4(e) show using electron energy loss spectroscopy (EELS) mapping that the elements are uniformly distributed throughout the nanorod, while Sn has a slight penetration gradient. Moreover, it is possible to observe from the high-angle annular dark-field scanning transmission electron microscopy (HAADF-STEM) image that the ion diffusion was very successful since there were no attached nanoparticles on the surface; it contains only external doping atoms, which are circled in Fig. 4(f). The co-doped photoelectrode showed a photocurrent increase of 62% relative to pristine hematite and a cathodic shift of 70 mV in V_{onset}, as seen in Fig. 4(g). The observed increased in the donor density [Fig. 4(h)], related to the generation of more Fe^{2+} ions or oxygen vacancies in the bulk, improved the Nb,Sn:Fe_2O_3 conductivity. By monitoring the charge separation efficiencies by comparing photo-oxidation currents of water and a hole scavenger, the authors realized that the successive modifications of Nb,Sn:Fe_2O_3 do explain the overall PEC response

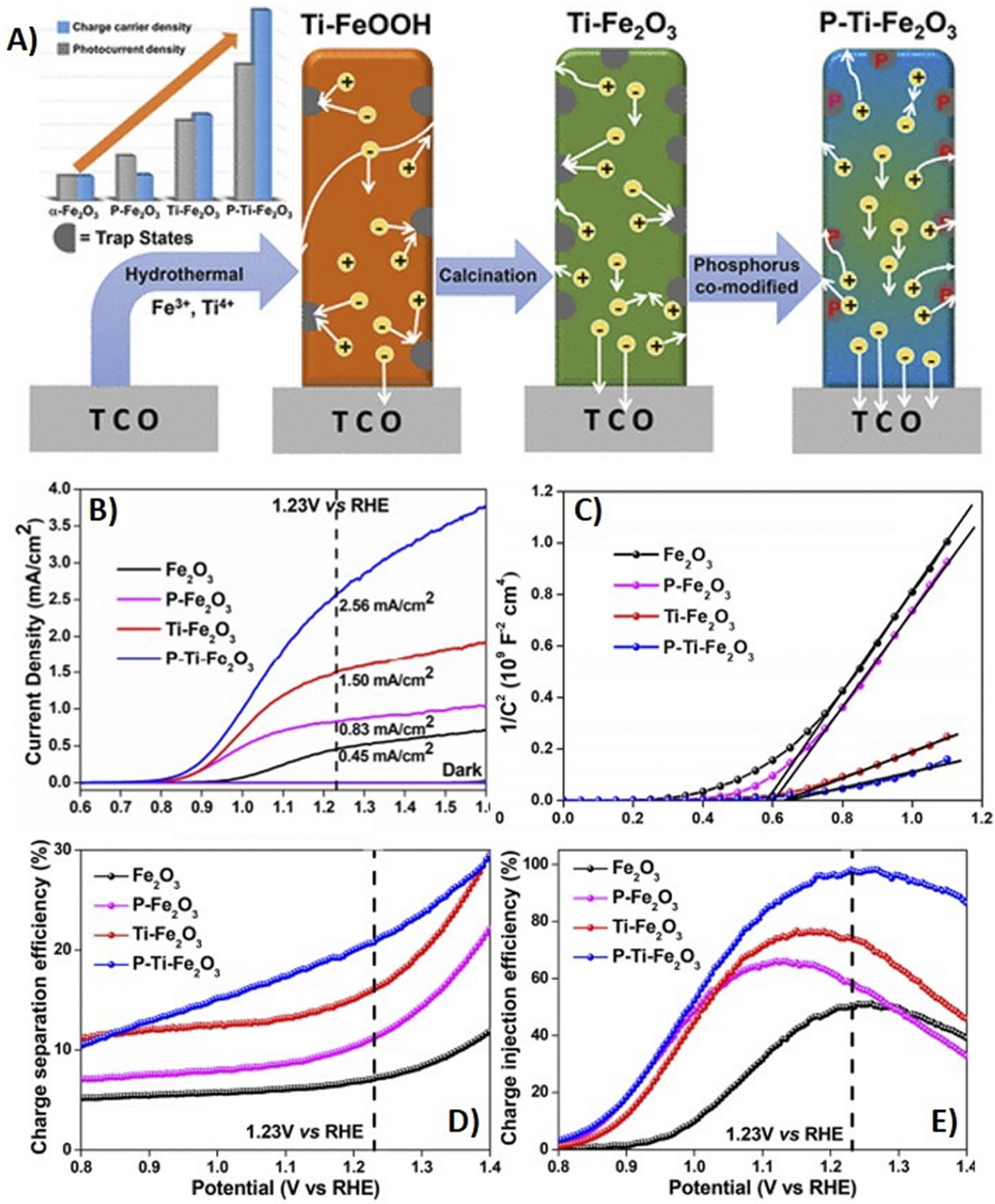

FIG. 3. (a) Schematic illustration of Ti–Fe_2O_3 and P–Ti–Fe_2O_3 photoanodes after sequential *in situ* doping of Ti and *ex situ* doping of P with their respective (b) photocurrent density, (c) Mott–Schottky plots, (d) charge separation efficiency (η_{sep}), and (e) charge injection efficiency (η_{inj}) of all the hematite photoanodes.[58] Reproduced with permission from Sahu *et al.*, ACS Appl. Energy Mater. **2**, 4325–4334 (2019). Copyright 2019 American Chemical Society.

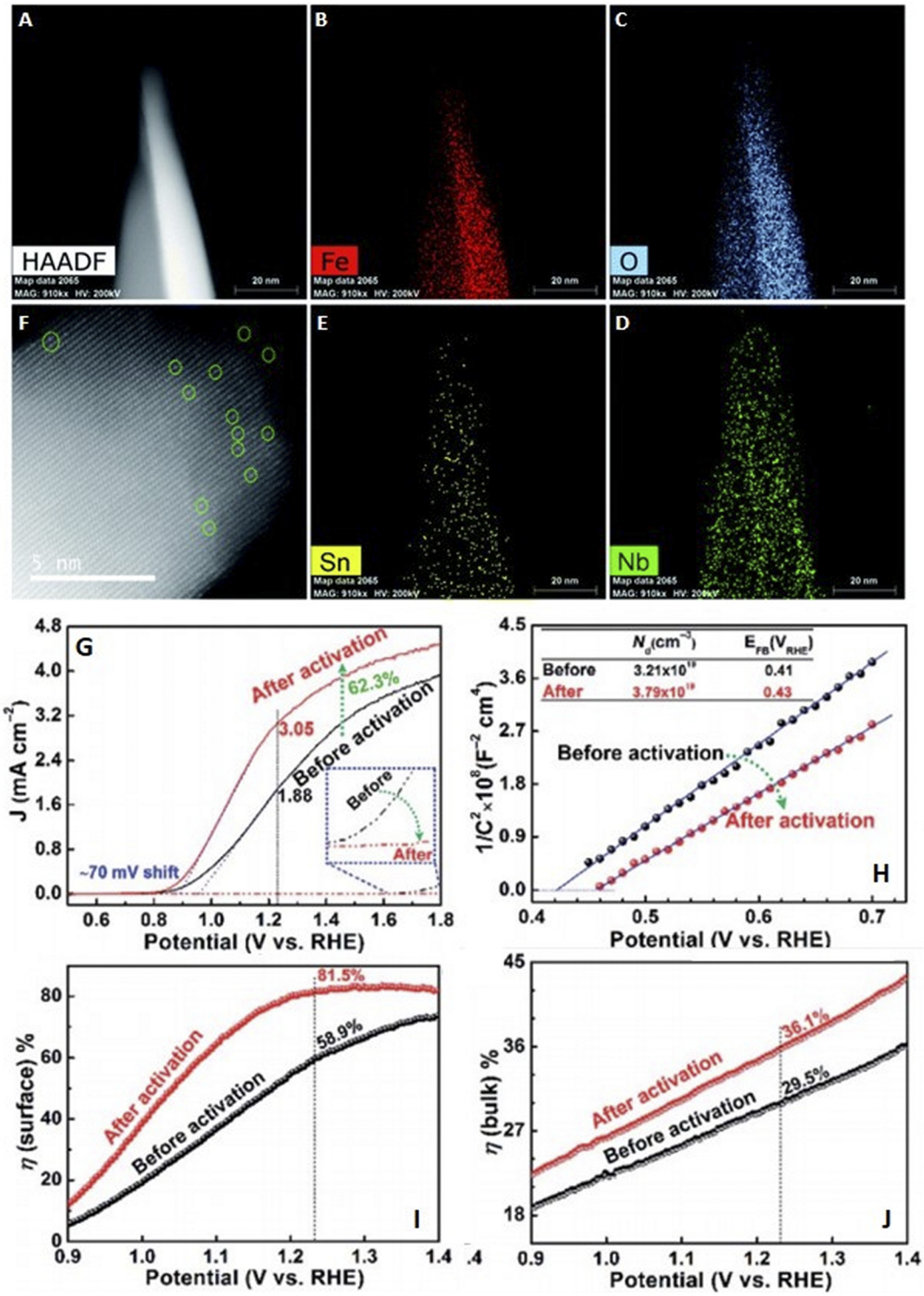

FIG. 4. (a) Scanning transmission electron microscopy (STEM) and (f) high-angle annular dark-field (HAADF-STEM) images of the synthesized Nb,Sn:Fe_2O_3 nanorods and [(b)–(e)] their corresponding EDX mappings of Fe, O, Nb, and Sn, respectively. (g) Photocurrent densities, (h) Mott–Schottky plots, (i) surface charge separation efficiency ($\eta_{surface}$), and (j) bulk charge separation efficiency (η_{bulk}) before and after the activation treatment.[59] Reproduced with permission from Zhang *et al.*, Chem. Sci. **10**, 10436–10444 (2019). Copyright 2019 Royal Society of Chemistry.

achieved, as they improved the charge separation efficiencies both on the surface ($\eta_{surface}$) and in the bulk (η_{bulk}), as shown in Figs. 4(i) and 4(j). Although the PEC activity of the photoanodes reported above is not as enhanced as expected, these studies provide strategic insights to increase the efficiency of charge separation and inspire the construction of new hematite-based systems.

B. Co-catalysts and passivating layers

Considering doping as the most commonly used mechanism for reducing bulk resistivity and increasing electronic transport, other pathways to overcome the known limitations in the charge separation processes at different interfaces of hematite-based photoelectrodes have already been considered. These losses can be alleviated by introducing an oxide layer (passivation layer) or by the presence of a co-catalyst. Thus, several studies have been proposed for the use of both strategies for PEC hematite devices, highlighting the fundamentally different operational mechanisms to improve charge separation and transfer processes.[60–62] Thin passivation layers, in forming heterojunctions with the semiconductor, can decrease the surface defect density reducing the recombination rate, increase the water oxidation reaction kinetics, and protect the semiconductor from chemical corrosion, improving their chemical stability and photoelectrochemical performance.[63,64] Several metal oxide compounds including Al_2O_3, TiO_2, Ga_2O_3, SiO_2, In_2O_3, and ZnO have been tested experimentally to modify the hematite photoanode surface showing a significant photocurrent improvement with a cathodic shift of V_{onset}.[11,65,66] Enthusiastic about the benefits of passivating layers, Hisatomi *et al.* performed a systematic screening of the effect of 13 group oxides as overlayers on the PEC performance of hematite photoelectrodes (M_2O_3/Fe_2O_3, M = Al, Ga, and In).[62] The largest cathodic shift in V_{onset} (200 mV) was obtained in a Ga_2O_3/Fe_2O_3 system which was attributed to its ability to decrease the surface trap density. By a simple method, hematite photoanodes were also easily passivated with TiO_2 overlayers as a strategy to favor the separation and charge transfer processes in the semiconductor–electrolyte interface, as shown in the work of Ahmed *et al.*[60] Photoelectrochemical measurements showed that the TiO_2 modified hematite photoanode exhibited a photocurrent increase of 4.5 relative to bare hematite along with a considerable cathodic shift. The TiO_2 layer acted as a passivation agent of the surface states, thereby reducing the surface electron–hole recombination while increasing the photovoltage and the band bending. Unlike the traditional passivating strategies, strategies such as sulfur- or boron-passivation have been employed to induce multistate species (ion terminations) in the hematite surface, which improve the carrier density, minimize the surface charge recombination, and accelerate the water oxidation kinetics at the solid–liquid interface simultaneously.[67]

To date, hematite photoelectrode architectures containing a passivating layer rely on the presence of a catalyst to improve the quality of the photoelectrode interface.[68,69] As commonly known, co-catalysts play an important function in PEC systems by reducing the redox overpotential for H_2 and O_2 evolution on their respective active sites, injecting holes from the semiconductor surface into the electrolyte.[1,70] In this context, catalysts such as CoPi, NiFe, FeOOH, NiOOH, and CoOOH have become an inevitable modification for improving the PEC water splitting response.[13] Typically, it has been observed that the presence of CoPi on the hematite surface can promote efficient charge separation and transport and may expand the depletion region, reducing, therefore, the surface electron–hole recombination.[71–74] Very recently, the study of Chen *et al.* proposed a rational arrangement of a stable and efficient hematite photoelectrode with the surface catalyzed by the cobalt molecular complex [$Co(dca)_2$, dca: dicyanamide] and protected by a thin layer of TiO_2.[75] Their data showed an improved and stabilized photoelectrochemical response compared to the pristine hematite. In this arrangement, the Co complex facilitated the charge transfer process at the semiconductor/electrolyte interface and accelerated the water oxidation reaction kinetics. The TiO_2 layer exhibited a dual role, inhibiting the surface defects and, thus, suppressing the carrier recombination, as well as protecting the complex Co-catalyst from detaching from the hematite surface, thus, stabilizing the PEC activity. This study highlighted the need for rational photoelectrode design for efficient pathways of the surface and interface charge carrier transfer processes, based on the synergy of metal oxides as passivation layers coupled with the presence of catalysts. Interestingly, Jeon *et al.* achieved a photocurrent density of 6 mA cm^{-2} at 1.23 V vs RHE for a hematite photoanode in elaborate and optimized surface modifications including H_2 treatment, a 3.5 nm-thick coating of TiO_2, and the deposition of the CoPi catalyst. For this system, the nanorod morphology allowed the radial hole transfer, the H_2 treatment increased the electrical conductivity, the TiO_2 passivation protected the hematite surface and reduced the surface recombination rates, and CoPi facilitated the interfacial reactions.[32] In the work of Ahn *et al.*, the presence of the Ti-doped SiOx layer on hematite mitigated the surface recombination losses and charge diffusion pathway, as well as increased the number of water oxidation active sites on the hematite surface.[76] After CoPi co-catalyst deposition, the photocurrent response of the Ti-(SiO_x/Fe_2O_3)/CoPi photoelectrode reached a value of 3.19 mA cm^{-2} at 1.23 V vs RHE, demonstrating the synergistic effect in this type of configuration by increasing the number of active sites and reducing the hole-diffusion pathway from the hematite to the electrolyte. Motivated to overcome the sluggish oxygen evolution reaction kinetics and drive charge transport, Ahn *et al.* reported a multistep preparation route that interconnected three functionalizations in a Zn–Co layered double hydroxide (LDH) decorated Ti/Sn co-doped α-Fe_2O_3 electrode, which resulted in a cathodic shift of over 300 mV and a PEC performance that achieved a photocurrent density of 2.0 mA cm^{-2} at 1.50 V vs RHE.[77] The doping reduced the recombination and led to a decrease in V_{onset}, while the synergistic interaction of the Zn^{2+}, Co^{2+}, and Co^{3+} from double hydroxide layers of Zn–Co LDH, by passivating surface states, facilitated the charge migration between the photoelectrode and the alkaline electrolyte. In the last years, NiFe layered double hydroxide (LDH) has been reported as a promising co-catalyst for hematite-based PEC photoanodes. Most of the studies showed a reduced V_{onset} and an enhanced photocurrent due to the fast and effective separation of photogenerated charge carriers and suppressed charge recombination provided by the NiFe layer.[78,79] Similarly, several studies addressing the use of other bifunctional oxide co-catalysts integrated with hematite arrays with remarkable PEC performances can be found in the literature.[80–84]

C. Plasmonic nanoparticles

Another possible strategy to further improve the hematite photocurrent and solve the trade-off between visible light absorption

and carrier collection efficiency is to incorporate plasmonic nanostructures to improve the solar energy conversion response. Plasmonic metal nanostructures can act by two mechanisms: (i) surface plasmon polaritons (SPPs), which are electromagnetic excitations existing at the surface of metallic films and (ii) localized surface plasmon resonance (LSPR), which is the collective stationary oscillation of surface electrons in metallic nanostructures. Using this strategy, the solar energy conversion efficiency of the semiconductor can occur by photonic enhancement or plasmonic energy-transfer enhancement.[85] In general, the SPP resonance modes exist simultaneously with the LSPR modes in hematite/metallic nanoparticle arrays, being the first mechanism located in the spectral range of UV to visible, while the other one covers the visible region for near-infrared (NIR) regions. Thus, by optimizing the resonance frequencies for specific spectral positions, a global improvement of the PEC arrangement can be obtained. The different origins of the SPP and LSPR modes, which combine and generate different responses in the photoconversion efficiency and an increase in the useful charge carrier lifetime in systems containing gold and hematite, were well discussed in the work of Wu's group. In this, the different ways of improving the efficiency of solar energy conversion are evidenced by experimental data and theoretical calculations, showing that the SPP effect increased the optical transmission by concentrating the incident light at energies above the band edge of hematite, while the LSPR created a clear field improvement at the metallic gold/hematite interface, facilitating the injection of electrons into the semiconductor.[85] The main contributions from plasmonic nanoparticles in hematite PEC devices include: efficient charge separation, improved light absorption in the visible region, pronounced surface catalytic activity, and increased bulk charge transport.[86–93] Herein, we highlighted some practical results based on traditional binary (metal/semiconductor) or ternary (metal/multisemiconductors) heterojunctions. Tofanello *et al.* opened a new discussion on Au-nanoparticle (NP)-supported on the hematite surface, which clearly promoted higher light absorption.[94] Surprisingly, the same trend was not observed in photoelectrochemical efficiency, suggesting that the plasmon effect is not a dominant phenomenon to drive photoelectrode performance, revealing a majority effect on charge transport and transfer properties. It was related that the coupling between a metal and a semiconductor can result in the formation of trap states at the interface, which promotes charge recombination and Fermi level pinning. Thus, undesirably, the hematite surface decorated with gold nanoparticles presented a negative effect on overall water photooxidation performance, as shown by Thimsen *et al.*[88] Indeed, the photocurrent decrease was attributed to the presence of surface states at the metal–semiconductor junction, which increased charge recombination. In addition, the authors reported that the Schottky junction between the interfaces limits open-circuit photovoltage and proposed an electronic isolation layer between the metal and the semiconductor, maximizing the metal semiconductor barrier height. Thus, carefully aligned with this strategy of plasmonic enhancement effects at the interfaces, thin metal oxide coatings or core–shell motif to protect the metallic core are being employed to increase the number of active sites and accelerate the charge injection or energy transfer.[95–100] In an attempt to control charge transfer across the plasmon–hematite junction, Li *et al.* proposed a rational arrangement based on metal–insulator–semiconductor heterostructures (Au@SiO_2-decorated α-Fe_2O_3 nanorod array) that would allow maximum PEC efficiency. The presence of the SiO_2 layer protecting the AuNPs was found to suppress the charge recombination, as well as maximize the metal–semiconductor barrier height, which resulted in a significant plasmon-driven photocurrent performance.[97] In another report, using the same previous ternary heterojunction, Thomann *et al.* coated gold nanostructures with a thin layer of SiO_2, which protected the metal from possible catalytic effects, while acting as a barrier preventing hot electron migration across the plasmonic–semiconductor interface, increasing, consequently, the system's PEC performance.[95] Another study that employed the concept of the ternary junction (Fe_2O_3/FeOOH/Au) showed that plasmonic nanoparticles along with akaganeite (beta-FeOOH) behaved as a unique "hole-depletion" layer, improving the PEC water oxidation response due to the cooperative synergy between charge separation and hole transfer.[101] In this dual co-catalytic system, the plasmonic nanoparticles injected more electrons to neutralize the holes while FeOOH trapped the holes and carried them to the solid–liquid interface efficiently. Although the literature has observed significant improvements using noble metals in hematite photoanodes (plasmonic hematite-based PEC devices), their practical applications are not strongly encouraged due to their scarcity and high cost.[102] Therefore, it is urgent to search alternative candidates to replace noble metals for PEC water splitting. In terms of work function and conductivity, Al, Ni, and Co metals are similar to noble metals and can, therefore, be used in trapping and transferring electrons in PEC reactions as well, since it is expected to form favorable energy band alignment for hot-carrier transfer at the interface.[103,104] Besides them, some transition metal nitrides, such as TiN and ZrN, are attracting attention as they have high temperature durability, chemical stability, corrosion resistance, and mechanical strength.[105] One of the major studies showing the plasmonic property of aluminum for hematite-based photoanodes was suggested by Ramadurgam *et al.*[106] In a systematic study, the authors proposed semiconductor–metal–metal oxide core-multishell (CMS) nanowires (Si–Al–Fe_2O_3), employing aluminum (Al) as a novel class of plasmonic material. When they evaluated the pristine Fe_2O_3, Si–Fe_2O_3 core shell (CS), Si–Au–Fe_2O_3 CMS, Si–Ag–Fe_2O_3 CMS, and Si–Al–Fe_2O_3 CMS architectures, the latter presented the largest absorbed integrated photon flux. In terms of photoelectrochemical response, Si–Al–Fe_2O_3 CMS exhibited values comparable to the analogous system Si–Ag–Fe_2O_3 CMS, reaching the remarkable photocurrent density of 11.8 mA cm^{-2}, which is about 93% of the theoretical maximum bulk alpha-Fe_2O_3 reported to date. These data suggest that under rational design conditions, plasmon resonance of aluminum may be beneficial. The presence of Al made the Fe_2O_3 outer shell remarkably increase the visible light absorption, acting as an electric field amplifier as well as exhibiting minimal recombination, favoring the charge transport near the electrolytic interface. Three years later, light absorption and near field enhancement properties of Al@Fe_2O_3 core shell hybrids (HNs) were studied theoretically by discrete dipole approximation (DDA) simulations.[107] To give even more reliability of the theoretical methodology used, the authors compared their results with those already published by Ramadurgam *et al.*[106] Overall, the improvement of light absorption by the presence of aluminum was attributed to the plasmon-induced energy transfer based on near field enhancement generated by the metal–semiconductor coupling. In addition, they observed that the

effect of parameters such as length, inner radius, and external radius of the HNs modifies the flux of absorbed photons, suggesting that the Al core can be tuned in the visible region by correctly adjusting the length of the HN. In addition, data from comparative systems showed that Al absorbed more light in the Fe_2O_3 shell than the noble metals Ag and Au. However, it is worth mentioning that despite the low cost, Al nanostructures, for example, cannot be employed on a large scale due to the explosive reactivity of the aluminum precursor with air and water, low melting point, low stability under alkaline conditions, and low thermal stability.[105,107] From the results presented above on the use of surface plasmon resonance in hematite-based photoelectrodes, it is clear that current applications should involve an architecture based on optimizing their morphologies, the type of metal–semiconductor coupling, and which component to use (be it another conductive metal oxide or a protective insulating layer) to mitigate the damaging effects of charge recombination. Therefore, researchers should consider all of these criteria to design novel noble metal–hematite photoelectrodes with high efficiency and stability.

D. Semiconductor heterojunctions

Despite the aforementioned methods for reducing the interface losses, recently, the construction of an engineered hierarchical interface of hematite has been established as a rational strategy to achieve band structure alignment to promote a positive balance between the parameters of Eq. (1). On a structural hierarchy scale, the next results show more complex hematite-based photoelectrode arrangements, in line with the most emerging trends for improving PEC. Compared to systems containing only one modifying element, these proposed systems tend to have superior PEC water oxidation performance due to synergistic effects caused by interactions of their components. In general, complex arrays are based on the presence of different components that minimize the deleterious effects of each interface (positively maximizing the η_{sep}, η_{inj}, and J_{ABS} parameters), especially other hematite-coupled metal oxides, due to the cascade electron transfer effect. The combination of modifications governing the improvement of hierarchical interface hematite devices should be aware of the photoelectrochemical response presented by each change or their synergism. For instance, Zhang *et al.* showed that the cocatalytic system consisting of multiple components, in the case of carbon nanodots (Cdots) and Co_3O_4 deposited in hematite, can have synergistic co-catalytic effects, causing an increase in the photocurrent density.[108] The hypothesis was that the two-step-two-electron reaction pathway and the enhanced surface reaction rate increased the solar water–oxidation activity. Their $C/Co_3O_4/Fe_2O_3$ photoanode showed a photocurrent density of 1.48 mA cm^{-2} at 1.23 V vs RHE, almost 80% higher than that of the pristine hematite photoanode. Adopting similar principles, in which the strategy was to simultaneously improve the charge transfer capacity and surface reaction kinetics, Shen's group successfully synthesized cobalt oxide (CoO_x) and carbon (C) modified hematite nanorod arrays.[113] The experimental analyses revealed that the CoO_x/C modified α-Fe_2O_3 exhibited an enhanced PEC performance in comparison to the CoO_x or C singly modified counterpart. The enhanced capacity created by the multifunctional modification was attributed to improved charge transfer ability and the accelerated electrode/electrolyte water oxidation reaction kinetics. The study performed by Tamirat *et al.* showed the combined effect of co-catalysts and surface treatment with Sn on the hematite surface to overcome the sluggish hole transfer and the charge transfer across the system interfaces.[69] The best PEC performance was obtained by the $Fe_2O_3/Fe_{2x}Sn_xO_3$/NiOOH photoanode with a photocurrent density of 1.73 mA cm^{-2} at 1.23 V vs RHE. The authors proposed that the $Fe2_xSn_xO_3$ (Sn^{4+} doped) passivating layer strongly inhibited the interfacial recombination by surface states, while NiOOH improved the charge transfer process across the passivated hematite and electrolyte interface. The transient photocurrent and EIS measurements showed an effective way to reduce interfacial recombination and enhance the charge transfer process across the semiconductor/electrolyte interface by employing surface passivation layers first and catalysts sequentially. A new approach to overcome the multiple charge limitations occurring in the bulk, interfaces, and surface of the hematite photoanode recently developed by Cho *et al.* deserves particular attention.[114] The combination of Ti-doped hematite, the insertion of a SnO_2 layer between the semiconductor and the FTO substrate, and the subsequent oxalic acid etching and FeOOH deposition effectively reduced the multiple electron/hole recombination pathways, leading to an improved photocurrent density at low bias potential. Tang *et al.* clarified the mechanism involved in charge transfers that occur in quaternary hematite compounds in two recent papers. The first one investigated the hierarchical ITO/Fe_2O_3/Fe_2TiO_5/FeNiOOH nanowires, in which the photoanode presented a photocurrent of 2.2 mA cm^{-2} at 1.23 V vs RHE, which is 10 times higher than that of pristine hematite.[27] After numerous investigations, the authors attributed the improvement in the photoelectrochemical response to the interfacial coupling of the system, in which the ITO promoted Sn doping, the Fe_2TiO_5 layer, in turn, increased the surface state density due to Ti, and the FeNiOOH nanodots improved the surface state sites. More recently, the same group incorporated a CoFe Prussian blue analog (CoFe-PBA) in core–shell Fe_2O_3/Fe_2TiO_5 nanowires and tested them in an acidic electrolyte (pH = 1).[109] The satisfactory photoelectrochemical response was attributed to the modified surface state density provided by the heterojunction arrangement which facilitated the charge transfer. For similar purposes, the experiments of Li *et al.* demonstrated that F-doping and NiOOH coating onto hematite photoanodes (NiOOH/Fe_2O_3/F–Fe_2O_3) resulted in an improved PEC performance due to the low surface trapping sites and efficient charge transfer through surface states.[110] The most current study, developed by Fu *et al.* and aligns with the latest methods of manufacturing efficient water splitting devices, was based on the strategy of exploring interface engineering for simultaneously reducing bulk and surface recombination in α-Fe_2O_3/Au/TiO_2 ternary photoanodes.[111] According to the data in Fig. 5(a), the photoelectrodes containing AuNPs exhibited greater η_{sep} than the pristine one, promoting the hole migration to the surface. By analyzing the charge injection efficiency (η_{inj}) from Fig. 5(b), the authors could confirm that TiO_2 behaved as a charge storage layer that facilitated the hole injection into the electrolyte for accelerating the water oxidation reaction. In the proposed configuration, the focus was to facilitate the charge migration at different interfaces, in which each constituent fulfills its role, as seen in Figs. 5(c)–5(f). First, the photogenerated holes were extracted from hematite and transported by the plasmonic nanoparticles to the Fe_2O_3/TiO_2 interface. After that, the photogenerated charges were injected by the ion-permeable TiO_2 overlayer into the electrolyte, catalyzing the water oxidation

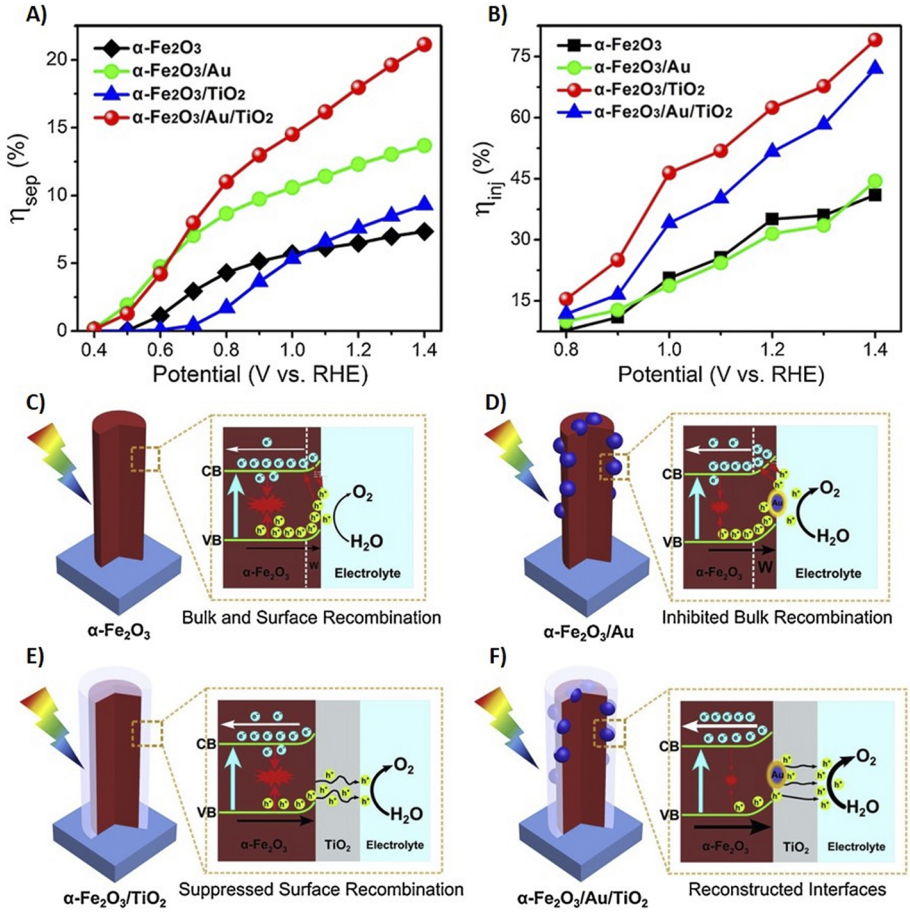

FIG. 5. (a) Charge separation efficiency (η_{sep}) and (b) charge injection efficiency (η_{inj}) of all the synthesized photoanodes, which are calculated by adding Na_2SO_3 as a hole scavenger into the electrolyte. Proposed charge transfer processes of different photoanodes: (c) α-Fe_2O_3, (d) α-Fe_2O_3/Au, (e) α-Fe_2O_3/TiO_2, and (f) α-Fe_2O_3/Au/TiO_2. The space-charge layer (SCL) region is marked with a dashed line and labeled W.[111] Reproduced with permission from Fu *et al.*, Appl. Catal., B **260**, 118206 (2020). Copyright 2020 Elsevier, Inc.

reactions. EIS measurements confirmed that the highest η_{sep} and η_{inj} were achieved by α-Fe_2O_3/Au/TiO_2 over the entire potential range demonstrating the success of the reconstructed interface strategy. Investigations with hierarchical interface constructions similar to the above mentioned systems reported that due to their engineered junctions, the metal is responsible for extracting photogenerated holes, while the second semiconductor layer efficiently injects them into the reaction medium.[112–114] In another case, a sandwiched configuration proposed by Kant *et al.* proved that the gold layer between the semiconductors plays a decisive role in facilitating the charge migration from the ZnO to the Fe_2O_3 conduction band due to the combined effect of the optimal band level alignment and SPR effect.[115] In summary together, the reports presented in this section show that to circumvent hematite limitations in which photoexcited charges are generated far away from a reactive surface and recombine rather than participate in the water splitting reactions, the rational construction of interfaces enables the optimization of a wide range of PEC devices.

III. CONCLUSIONS AND OUTLOOK

In recent years, research studies focusing on the development of highly efficient and stable photoanodes have been steadily expanding, and the progress mentioned in this perspective has been limited to highlighting only a selected portion of these contributions. It is clear that hematite-based photoanode manufacturing relies not only on material design but also on fully integrated PEC configurations. In this perspective, we pointed out the latest progress in hierarchical interface engineering of hematite-based PEC devices, with their corresponding charge transfer processes, which included: (i) dopant incorporation/segregation to overcome the poor electrical conductivity and improve the charge carriers' transfer; (ii) coupling semiconductors with passivating or co-catalyst layers to reduce the electron–hole recombination rate and favor the charge transport at the hematite/electrolyte interface, respectively; (iii) the insertion of metallic nanostructures (noble or non-noble metals) to improve the use of sunlight and boost the separation and transport of electron–hole pairs; (iv) the formation of multicomponent heterojunctions to improve sunlight utilization and improve the separation/transport of a photogenerated charge in a synergistic charge transfer effect. It is anticipated that the hierarchical interface engineering processes listed in this article will enable more effective strategies to significantly improve hematite-based PEC performance, as they can overcome the known shortcomings found in a hematite PEC device simultaneously, as summarized in Fig. 6 which presents a compiled overview of the rational design of heterojunctions to enable

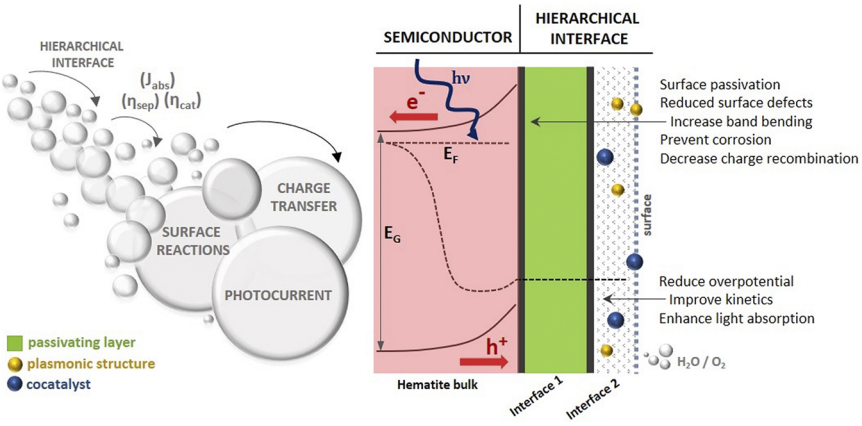

FIG. 6. Schematic illustration of the balance of the expected cascade effects of surface and interface engineering (left) and simulation of the photoelectrode construction interfaces with their respective benefits (right) for photoelectrochemical oxidation.[20] Adapted with permission from Kuang *et al.*, Joule **11**, 290–305 (2017). Copyright 2017 Elsevier, Inc.

the transfer of the photogenerated charge across the interfaces by optimizing n_{sep} and n_{inj} and, consequently, improving the photoelectrochemical efficiency. The constituents can be employed to mitigate the deleterious effects of the solid–solid and solid–liquid interfaces to achieve a PEC efficiency that justifies its practical operations. For this, the band structures of the semiconductors involved must be correctly positioned and the photocatalytic responses produced by the different constituents must be compatible, presenting a synergistic effect. It is obvious that many promising results have been achieved in this field, but it is worth mentioning that the practical efficiency of the photoelectrochemical reaction in hematite photoanodes is still limited and the industrialization and commercialization of these photoanodes still require additional studies. The current scenario shows us that major research efforts should be focused on some central aspects. Among them, one can reinforce the need to invest time and resources in the search for facile, cost-effective, and environmentally friendly synthetic methods for large-scale fabrication of high-performance hematite-based photoanodes. Moreover, hematite photoanode construction strategies should be pursued to facilitate paths for efficient charge migration through interface engineering. The photoanodes must simultaneously meet the requirements of low surface trapping sites, efficient charge separation, and injection efficiency. In this context, studies of ternary or quaternary visible light-responsive heterojunctions have been shown to be efficient, since they can overcome many of the drawbacks faced in the energy conversion process. Thus, it is emphasized that the rational engineering of heterojunctions can open a new avenue for the fabrication and manufacturing of the next generation of low-cost, highly efficient, and stable PEC materials and devices. Finally, the latest advances in experimental (i.e., *in situ*/operando x-ray spectroscopies[116]) as well as theoretical (i.e., machine learning[117]) methods should ultimately unravel better atomic-scale fundamental knowledge for direct correlation between the structure and efficiency, thus, providing scientists and engineers the ideal conditions to fabricate novel devices based on hematite nanorod arrays with high stability and high performance.

ACKNOWLEDGMENTS

The authors acknowledge the support from the São Paulo Research Foundation [Project Nos. 2016/01000-2 and 2019/01977-4, Fundação de Amparo à Pesquisa do Estado de São Paulo (FAPESP)], the National Science Foundation of China (NSFC), the Outstanding Talent Program of Shaanxi Province, the State Key Laboratory for Multiphase Flow in Power Engineering, and the School of Energy & Power Engineering at Xi'an Jiaotong University.

REFERENCES

[1] N. Beerman, L. Vayssieres, S. E. Lindquist, and A. Hagfeldt, J. Electrochem. Soc. **147**, 2456–2461 (2000).
[2] B. Iandolo, B. Wickman, I. Zorić, and A. Hellman, J. Mater. Chem. A **3**, 16896–16912 (2015).
[3] Gurudayal, P. S. Bassi, T. Sritharan, and L. H. Wong, J. Phys. D: Appl. Phys. **51**, 473002 (2018).
[4] J. H. Kim, D. Hansora, P. Sharma, J.-W. Jang, and J. S. Lee, Chem. Soc. Rev. **48**, 1908–1971 (2019).
[5] P. Tang and J. Arbiol, Nanoscale Horiz. **4**, 1256–1276 (2019).
[6] S. Shen, J. Mater. Res. **29**, 29–46 (2014).
[7] S. Shen, S. A. Lindley, X. Chen, and J. Z. Zhang, Energy Environ. Sci. **9**, 2744–2775 (2016).
[8] A. E. Nogueira, M. R. Santos Soares, J. B. Souza Junior, C. A. Ospina Ramirez, F. L. Souza, and E. R. Leite, J. Mater. Chem. A **7**, 16992–16998 (2019).
[9] Y. He, T. Hamann, and D. Wang, Chem. Soc. Rev. **48**, 2182–2215 (2019).
[10] L. Vayssieres, C. Sathe, S. M. Butorin, D. K. Shuh, J. Nordgren, and J. Guo, Adv. Mater. **17**, 2320–2323 (2005).
[11] K. Wu and T. Lian, Chem. Soc. Rev. **45**, 3781–3810 (2016).
[12] K. M. Rosso, D. M. A. Smith, and M. Dupuis, J. Chem. Phys. **118**, 6455 (2003).
[13] J. Zhang and S. Eslava, Sustainable Energy Fuels **3**, 1351–1364 (2019).
[14] W. M. Carvalho, Jr., L. Mendonça-Ferreira, F. N. Costa, F. F. Ferreira, D. N. F. Muche, R. A. Tofanello, R. H. R. Castro, and F. L. Souza, J. Alloys Compd. **799**, 83–88 (2019).
[15] N. M. Ito, W. M. Carvalho, Jr., D. N. F. Muche, R. H. R. Castro, G. M. Dalpian, and F. L. Souza, Phys. Chem. Chem. Phys. **19**, 25025–25032 (2017).
[16] A. M. Xavier, F. F. Ferreira, and F. L. Souza, RSC Adv. **4**, 17753–17759 (2014).
[17] D. Wang, Y. Zhang, C. Peng, J. Wang, Q. Huang, S. Su, L. Wang, W. Huang, and C. Fan, Adv. Sci. **2**, 1500005 (2015).
[18] F. L. Souza, An. Acad. Bras. Cienc. **90**, 745–762 (2018).
[19] X.-T. Xu, L. Pan, X. Zhang, L. Wang, and J.-J. Zou, Adv. Sci. **6**, 1801505 (2019).
[20] Y. Kuang, T. Yamada, and K. Domen, Joule **1**, 290–305 (2017).
[21] S. Shen, M. Li, L. Guo, J. Jiang, and S. S. Mao, J. Colloid Interface Sci. **427**, 20–24 (2014).
[22] A. Tsyganok, D. Klotz, K. D. Malviya, A. Rothschild, and D. A. Grave, ACS Catal. **8**, 2754–2759 (2018).

[23]S.-S. Yi, B.-R. Wulan, J.-M. Yan, and Q. Jiang, Adv. Funct. Mater. **29**, 1801902 (2019).
[24]H. Zhang, W. Y. Noh, F. Li, J. H. Kim, H. Y. Jeong, and J. S. Lee, Adv. Funct. Mater. **29**, 1805737 (2019).
[25]C. Li, Z. Luo, T. Wang, and J. Gong, Adv. Mater. **30**, 1707502 (2018).
[26]K. H. Ye, H. Li, D. Huang, S. Xiao, W. Qiu, M. Li, Y. Hu, W. Mai, H. Ji, and S. Yang, Nat. Commun. **10**, 3687 (2019).
[27]P. Tang, H. Xie, C. Ros, L. Han, M. Biset-Peiró, Y. He, W. Kramer, A. P. Rodríguez, E. Saucedo, J. R. Galán-Mascarós, T. Andreu, J. R. Morante, and J. Arbiol, Energy Environ. Sci. **10**, 2124–2136 (2017).
[28]L. Wang, T. Nakajima, and Y. Zhang, J. Mater. Chem. A **7**, 5258–5265 (2019).
[29]D. Wu and Z. Zhang, Electrochim. Acta **282**, 48–55 (2018).
[30]J. W. Park, M. A. Mahadik, H. Ma, G. W. An, H. H. Lee, S. H. Choi, W.-S. Chae, H.-S. Chung, and J. S. Jang, ACS Sustainable Chem. Eng. **7**, 6947–6958 (2019).
[31]C. V. Reddy, I. N. Reddy, A. Sreedhar, and J. Shim, Appl. Surf. Sci. **488**, 629–638 (2019).
[32]T. H. Jeon, G.-H. Moon, H. Park, and W. Choi, Nano Energy **39**, 211–218 (2017).
[33]M. R. S. Soares, R. H. Gonçalves, I. C. Nogueira, J. Bettini, A. J. Chiquito, and E. R. Leite, Phys. Chem. Chem. Phys. **18**, 21780–21788 (2016).
[34]K. Sivula, F. Le Formal, and M. Grätzel, ChemSusChem **4**, 432–449 (2011).
[35]X. Zhang, X. Wang, X. Yi, J. Ye, and D. Wang, ACS Sustainable Chem. Eng. **7**, 5420–5429 (2019).
[36]Y. Yang, M. Forster, Y. Ling, G. Wang, T. Zhai, Y. Tong, A. J. Cowan, and Y. Li, Angew. Chem. **128**, 3464 (2016).
[37]M. Pyeon, T.-P. Ruoko, J. Leduc, Y. Gönüllü, M. Deo, N. V. Tkachenko, and S. Mathur, J. Mater. Res. **33**, 455–466 (2018).
[38]G. Liu, S. K. Karuturi, H. Chen, L. Spiccia, H. H. Tan, C. Jagadish, D. Wang, A. N. Simonov, and A. Tricoli, Nano Energy **53**, 745–752 (2018).
[39]W. Si, F. Haydous, U. Babic, D. Pergolesi, and T. Lippert, ACS Appl. Energy Mater. **2**, 5438–5445 (2018).
[40]S. Shen, P. Guo, D. A. Wheeler, J. Jiang, S. A. Lindley, C. X. Kronawitter, J. Z. Zhang, L. Guo, and S. S. Mao, Nanoscale **5**, 9867–9874 (2013).
[41]S. Shen, C. X. Kronawitter, J. Jiang, S. S. Mao, and L. Guo, Nano Res. **5**, 327–336 (2012).
[42]S. Shen, J. Jiang, P. Guo, C. X. Kronawitter, S. S. Mao, and L. Guo, Nano Energy **1**, 732–741 (2012).
[43]S. A. Carminati, A. N. Barbosa, A. L. M. Freitas, F. L. Freire, Jr., F. L. Souza, and A. F. Nogueira, J. Catal. **372**, 109–118 (2019).
[44]Y. Fu, C.-L. Dong, W.-Y. Lee, J. Chen, P. Guo, L. Zhao, and S. Shen, ChemNanoMat **2**, 704–711 (2016).
[45]S. Shen, J. Zhou, C. L. Dong, Y. Hu, E. N. Tseng, P. Guo, L. Guo, and S. S. Mao, Sci. Rep. **4**, 6627 (2014).
[46]Q. Zhu, C. Yu, and X. Zhang, J. Energy Chem. **35**, 30–36 (2019).
[47]A. Annamalai, H. H. Lee, S. H. Choi, S. Y. Lee, E. Gracia-Espino, A. Subramanian, J. Park, K. J. Kong, and J. S. Jang, Sci. Rep. **6**, 23183 (2016).
[48]A. G. Hufnagel, H. Hajiyani, S. Zhang, T. Li, O. Kasian, B. Gault, B. Breitbach, T. Bein, D. Fattakhova-Rohlfing, C. Scheu, and R. Pentcheva, Adv. Funct. Mater. **28**, 1804472 (2018).
[49]C. X. Kronawitter, I. Zegkinoglou, S.-H. Shen, P. Liao, I. S. Cho, O. Zandi, Y.-S. Liu, K. Lashgari, G. Westin, J.-H. Guo, F. J. Himpsel, E. A. Carter, X. L. Zheng, T. W. Hamann, B. E. Koel, S. S. Mao, and L. Vayssieres, Energy Environ. Sci. **7**, 3100–3121 (2014).
[50]A. L. M. Freitas and F. L. Souza, Nanotechnology **28**, 454002 (2017).
[51]T.-T. Kong, J. Huang, X.-G. Jia, W.-Z. Wang, and Y. Zhou, Appl. Surf. Sci. **486**, 312–322 (2019).
[52]J. Wang, N. H. Perry, L. Guo, L. Vayssieres, and H. L. Tuller, ACS Appl. Mater. Interfaces **11**, 2031–2041 (2019).
[53]M. R. S. Soares, C. A. R. Costa, E. M. Lanzoni, J. Bettini, C. A. O. Ramirez, F. L. Souza, E. Longo, and E. R. Leite, Adv. Electron. Mater. **5**, 1900065 (2019).
[54]Gurudayal, R. A. John, C. Yi, C. Shi, M. C. Scott, S. A. Veldhuis, A. M. Minor, S. M. Zakeeruddin, L. H. Wong, M. Grätzel, and N. Mathews, ChemSusChem **10**, 2449 (2017).
[55]J. Su, J. Wang, C. Liu, B. Feng, Y. Chen, and L. Guo, RSC Adv. **6**, 101745–101751 (2016).
[56]J. Wang, C. Du, Q. Peng, J. Yang, Y. Wen, B. Shan, and R. Chen, Int. J. Hydrogen Energy **42**, 29140–29149 (2017).
[57]A. Cots and R. Gómez, Appl. Catal., B **219**, 492–500 (2017).
[58]T. K. Sahu, A. K. Shah, A. Banik, and M. Qureshi, ACS Appl. Energy Mater. **2**, 4325–4334 (2019).
[59]H. Zhang, J. H. Park, W. J. Byun, M. H. Song, and J. S. Lee, Chem. Sci. **10**, 10436–10444 (2019).
[60]M. G. Ahmed, I. E. Kretschmer, T. A. Kandiel, A. Y. Ahmed, F. A. Rashwan, and D. W. Bahnemann, ACS Appl. Mater. Interfaces **7**, 24053–24062 (2015).
[61]F. Le Formal, N. Tétreault, M. Cornuz, T. Moehl, M. Grätzel, and K. Sivula, Chem. Sci. **2**, 737–743 (2011).
[62]T. Hisatomi, F. Le Formal, M. Cornuz, J. Brillet, N. Tétreault, K. Sivula, and M. Grätzel, Energy Environ. Sci. **4**, 2512–2515 (2011).
[63]R. Liu, Z. Zheng, J. Spurgeon, and X. Yang, Energy Environ. Sci. **7**, 2504–2517 (2014).
[64]D. Bae, B. Seger, P. C. K. Vesborg, O. Hansen, and I. Chorkendorff, Chem. Soc. Rev. **46**, 1933–1954 (2017).
[65]J. Wang, B. Feng, J. Su, and L. Guo, ACS Appl. Mater. Interfaces **8**, 23143–23150 (2016).
[66]L. Mao, Y.-C. Huang, Y. Fu, C.-L. Dong, and S. Shen, Sci. Bull. **64**, 1262–1271 (2019).
[67]H. Lan, A. Wei, H. Zheng, X. Sun, and J. Zhong, Nanoscale **10**, 7033–7039 (2018).
[68]S. Hu, N. S. Lewis, J. W. Ager, J. Yang, J. R. McKone, and N. C. Strandwitz, J. Phys. Chem. C **119**, 24201–24228 (2015).
[69]A. G. Tamirat, A. A. Dubale, W.-N. Su, H.-M. Chen, and B.-J. Hwang, Phys. Chem. Chem. Phys. **19**, 20881–20890 (2017).
[70]J. Deng, Q. Zhang, K. Feng, H. Lan, J. Zhong, M. Chaker, and D. Ma, ChemSusChem **11**, 3783 (2018).
[71]L. Fu, H. Yu, C. Zhang, Z. Shao, and B. Yi, Electrochim. Acta **136**, 363–369 (2014).
[72]T. Wang, H.-T. Hung, Y.-R. Cheng, M.-C. Huang, Y.-K. Hsieh, and C.-F. Wang, RSC Adv. **6**, 28236–28247 (2016).
[73]Y. Ma, A. Kafizas, S. R. Pendlebury, F. Le Formal, and J. R. Durrant, Adv. Funct. Mater. **26**, 4951–4960 (2016).
[74]G. M. Carroll and D. R. Gamelin, J. Mater. Chem. A **4**, 2986–2994 (2016).
[75]X. Chen, Y. Fu, T. Kong, Y. Shang, F. Niu, Z. Diao, and S. Shen, Eur. J. Inorg. Chem. **2019**, 2078–2085.
[76]H.-J. Ahn, K.-Y. Yoon, M.-J. Kwak, and J.-H. Jang, Angew. Chem., Int. Ed. **55**, 9922 (2016).
[77]H.-J. Ahn, A. Goswami, F. Riboni, S. Kment, A. Naldoni, S. Mohajernia, R. Zboril, and P. Schmuki, ChemSusChem **11**, 1873–1879 (2018).
[78]Y. B. Park, J. H. Kim, Y. J. Jang, J. H. Lee, M. H. Lee, B. J. Lee, D. H. Youn, and J. S. Lee, ChemCatChem **11**, 443 (2019).
[79]Y. Zhu, X. Zhao, J. Li, H. Zhang, S. Chen, W. Han, and D. Yang, J. Alloys Compd. **764**, 341–346 (2018).
[80]L. Liardet, J. E. Katz, J. Luo, M. Grätzel, and X. Hu, J. Mater. Chem. A **7**, 6012–6020 (2019).
[81]H. Hajibabaei, A. R. Schon, and T. W. Hamann, Chem. Mater. **29**, 6674–6683 (2017).
[82]C. Wang, X. Long, S. Wei, T. Wang, F. Li, L. Gao, Y. Hu, S. Li, and J. Jin, ACS Appl. Mater. Interfaces **11**, 29799–29806 (2019).
[83]X. Yu, J. Liu, W. Yin, T. Wang, L. Quan, Y. Ran, J. Cui, L. Wang, and Y. Zhang, Appl. Surf. Sci. **492**, 264–271 (2019).
[84]G. Wang, B. Wang, C. Su, D. Li, L. Zhang, R. Chong, and Z. Chang, J. Catal. **359**, 287–295 (2018).
[85]J. Li, S. K. Cushing, P. Zheng, F. Meng, D. Chu, and N. Wu, Nat. Commun. **4**, 2651 (2013).
[86]T. G. U. Ghobadi, A. Ghobadi, E. Ozbay, and F. Karadas, ChemPhotoChem **2**, 161 (2018).

[87]B. Chen, W. Fan, B. Mao, H. Shen, and W. Shi, Dalton Trans. **46**, 16050–16057 (2017).
[88]E. Thimsen, F. Le Formal, M. Grätzel, and S. C. Warren, Nano Lett. **11**, 35–43 (2011).
[89]L. Mascaretti, A. Dutta, Š. Kment, V. M. Shalaev, A. Boltasseva, R. Zbořil, and A. Naldoni, Adv. Mater. **31**, 1805513 (2019).
[90]G. Liu, K. Du, J. Xu, G. Chen, M. Gu, C. Yang, K. Wang, and H. Jakobsen, J. Mater. Chem. A **5**, 4233–4253 (2017).
[91]Q. Zhang, D. Thrithamarassery Gangadharan, Y. Liu, Z. Xu, M. Chaker, and D. Ma, J. Mater. **3**, 33–50 (2017).
[92]J. B. Lee, S. Choi, J. Kim, and Y. S. Nam, Nano Today **16**, 61–81 (2017).
[93]A. Naldoni, F. Riboni, U. Guler, A. Boltasseva, V. M. Shalaev, and A. V. Kildishev, Nanophotonics **5**, 112–133 (2016).
[94]A. Tofanello, A. L. M. Freitas, W. M. Carvalho, Jr., T. Salminen, T. Niemi, and F. L. Souza, J. Phys. Chem. C **124**, 6171–6179 (2020).
[95]I. Thomann, B. A. Pinaud, Z. Chen, B. M. Clemens, T. F. Jaramillo, and M. L. Brongersma, Nano Lett. **11**, 3440–3446 (2011).
[96]N. Wu, Nanoscale **10**, 2679–2696 (2018).
[97]C. Li, P. Wang, H. Li, M. Wang, J. Zhang, G. Qi, and Y. Jin, Nanoscale **10**, 14290–14297 (2018).
[98]Z. Xu, Z. Fan, Z. Shi, M. Li, J. Feng, L. Pei, C. Zhou, J. Zhou, L. Yang, W. Li, G. Xu, S. Yan, and Z. Zou, ChemSusChem **11**, 237–244 (2018).
[99]Y. Liu, Z. Xu, M. Yin, H. Fan, W. Cheng, L. Lu, Y. Song, J. Ma, and X. Zhu, Nanoscale Res. Lett. **10**, 374 (2015).
[100]I. Khan and A. Qurashi, ACS Sustainable Chem. Eng. **6**, 11235–11245 (2018).
[101]L. Wang, H. Hu, N. T. Nguyen, Y. Zhang, P. Schmuki, and Y. Bi, Nano Energy **35**, 171–178 (2017).
[102]S. Kim, J.-M. Kim, J.-E. Park, and J.-M. Nam, Adv. Mater. **30**, 1704528 (2018).
[103]A. Naldoni, U. Guler, Z. Wang, M. Marelli, F. Malara, X. Meng, L. V. Besteiro, A. O. Govorov, A. V. Kildishev, A. Boltasseva, and V. M. Shalaev, Adv. Opt. Mater. **5**, 1601031 (2017).
[104]Y. Chen, X. Xin, N. Zhang, and Y.-J. Xu, Part. Part. Syst. Charact. **34**, 1600357 (2017).
[105]E. R. Encina and E. A. Coronado, J. Phys. Chem. C **122**, 4589–4599 (2018).
[106]S. Ramadurgam, T.-G. Lin, and C. Yang, Nano Lett. **14**, 4517–4522 (2014).
[107]E. R. Encina, N. Passarelli, and E. A. Coronado, RSC Adv. **7**, 2857–2868 (2017).
[108]P. Zhang, T. Wang, X. Chang, L. Zhang, and J. Gong, Angew. Chem., Int. Ed. **55**, 5851–5855 (2016).
[109]P. Y. Tang, L. J. Han, F. S. Hegner, P. Paciok, M. Biset-Peiró, H. C. Du, X. K. Wei, L. Jin, H. B. Xie, Q. Shi, T. Andreu, M. Lira-Cantú, M. Heggen, R. E. Dunin-Borkowski, N. López, J. R. Galán-Mascarós, J. R. Morante, and J. Arbiol, Adv. Energy Mater. **9**, 1901836 (2019).
[110]F. Li, J. Li, L. Gao, Y. Hu, X. Long, S. Wei, C. Wang, J. Jin, and J. Ma, J. Mater. Chem. A **6**, 23478–23485 (2018).
[111]Y. Fu, C.-L. Dong, W. Zhou, Y.-R. Lu, Y.-C. Huang, Y. Liu, P. Guo, L. Zhao, W.-C. Chou, and S. Shen, Appl. Catal., B **260**, 118206 (2020).
[112]A. Verma, A. Srivastav, S. A. Khan, V. Rani Satsangi, R. Shrivastav, D. Kumar Avasthi, and S. Dass, Phys. Chem. Chem. Phys. **19**, 15039–15049 (2017).
[113]M. Wang, M. Wang, Y. Fu, and S. Shen, Chin. Chem. Lett. **28**, 2207–2211 (2017).
[114]I. S. Cho, H. S. Han, M. Logar, J. Park, and X. Zheng, Adv. Energy Mater. **6**, 1501840 (2016).
[115]R. Kant, S. Pathak, and V. Dutta, Sol. Energy Mater. Sol. Cells **178**, 38–45 (2018).
[116]C. L. Dong and L. Vayssieres, Chem. - Eur. J. **24**, 18356–18373 (2018).
[117]K. T. Butler, D. W. Davies, H. Cartwright, O. Isayev, and A. Walsh, Nature **559**, 547–555 (2018).